Creep-induced phase transformations in furnace cooled Zn–Al alloy

Y.H. ZHU
Instituto de Investigaciones en Materiales, Universidad Nacional Autónoma de México, México, DF, Mexico

E. OROZCO
Instituto de Fisica, Universidad Nacional Autónoma de México, México, DF, Mexico

S. MURPHY
Aston University, Birmingham B4 7ET, UK

Phase transformation and microstructural change of a furnace-cooled eutectoid Zn–Al alloy specimen (76 wt % Zn–22 wt % Al–2 wt % Cu) were investigated during creep testing by using scanning electron microscopy and X-ray diffraction techniques. Creep-induced decomposition of a metastable η'_T phase and a four-phase transformation, $\alpha + \varepsilon \rightarrow T' + \eta$, occurred during the creep testing. Also microstructural change was observed from a lammellar structure partially into a spheroidized structure in the rupture part of the furnace-cooled alloy. The mechanism of the creep rupture of the furnace-cooled eutectoid Zn–Al alloy was also discussed.

1. Introduction

Zn–Al-based alloys are being applied in many industrial applications because of their excellent combination of good castability, mechanical properties and superplasticity. However, there are some practical difficulties, such as poor impact property and tensile creep behaviour, limited service temperature due to the low melting point, and dimensional instability (e.g., early stage of shrinkage and expansion during the prolonged ageing) for most cast Zn–Al-based alloys. The elevated-temperature mechanical properties, such as tensile creep resistance and impact property, become more important for practical applications.

Major efforts have been made to evaluate the creep resistance of the alloys with various chemical compositions at different temperatures [1–3]. Rare reports have been published on the microstructure dependence of the tensile creep properties. In order to understand the mechanism of tensile creep behaviour better, an extensive research programme on the tensile creep behaviour and associated phase transformation and microstructural change has recently been carried out on the thermal and thermomechanically treated eutectoid Zn–Al alloy, based on the systematic investigation on phase relationships of Zn–Al-based alloys of various compositions (Al–rich, monotectoid and eutectoid compositions) under different thermal and thermomechanical treatments, such as solution-treatment-quenched, cast, hot extrusion and weld processes [4–18].

The present work will report some results of microstructural change and phase transformation in a furnace-cooled eutectoid Zn–Al alloy under tensile creep.

2. Experimental procedure

A cast ingot of the eutectoid alloy 76 wt% Zn–22 wt % Al–2 wt % Cu was prepared from high-purity materials (99.99% Zn, 99.99% Al and 99.99% Cu) and melted in a graphite crucible, in an induction furnace. The melt was degassed with zinc chloride ($ZnCl_2$) and cast at 700 °C into a pre-heated mild steel mould. The cast ingot was solution treated at 350 °C for 4 days and then furnace cooled at room temperature.

The furnace-cooled ingot was machined into specimens of 6 mm diameter with 35 mm gauge length for creep test and specimens of 10 mm diameter with 50 mm gauge length for tensile testing. The creep test was carried out under stress of 30 MPa on a Satec model M3 constant-load creep machine. The temperature of the creep test was controlled at 150 ± 2 °C. Strain was measured with a Scheauifz DC-E 1000 LUDT with a linear range of ± 25.4 mm. The tensile testing was carried out at a cross-head speed of 7.00×10^{-3} mm s^{-1} on an Instron machine. The temperature of the tensile testing was controlled at 100 ± 2 °C. A chart recorder recorded automatically the load and the resulting extension of the specimens being tensile tested: on the basis of this, the engineering stress–strain curves were plotted.

Standard metallographic examination was carried out on both bulk part and rupture part of the ground and alumina polished specimen in a scanning electron microscope using a back-scattered electron image to attain atomic number contrast. X-ray diffraction examinations were carried out on various parts of the specimen: the bulk part, the rupture part and the overlapping zone of the transitional part and rupture

0022–2461

part after creep testing at 150 °C. A Philips X-ray diffractometer was employed with nickel-filtered Cu K_α radiation, at a scanning speed of 1° min^{-1}. The characteristic X-ray diffraction was collected within the diffraction angle 2θ range from 35° to 47°.

3. Results

3.1. Creep behaviour of the furnace-cooled alloy

A typical creep curve for the furnace-cooled eutectoid Zn–Al alloy is shown in Fig. 1. A fairly high strain at rupture was measured at 135.0%. The minimum creep rate of the furnace-cooled alloy was 8.7×10^{-4} s^{-1} under a stress of 30 MPa at 150 °C. The time at rupture was 2177 s. In comparison, the stress–strain curve of the tensile specimen was obtained in the tensile testing at a cross-head speed of 7.00×10^{-3} mm s^{-1} and 100 °C, as shown in Fig. 2. The tensile specimen ruptured when the strain reached 70.0% with a stress at rupture of 15.20 MPa. The ultimate tensile strength and the 0.2% proof stress of the furnace-cooled alloy were 68.59 MPa and 52.76 MPa, respectively.

3.2. X-ray diffraction examination

The X-ray diffractograms of various parts, namely the bulk part, the joint parts of the neck zone and the rupture part, of the specimen after creep test are shown in Fig. 3.

The bulk part of the specimen consisted of three phases α, ε and η'_T after the creep test at 150 °C, where α was Al-rich face-centred-cubic (f.c.c.) phase, ε was hexagonal close-packed (h.c.p.) $CuZn_4$ phase and η'_T was a Zn-rich metastable phase of h.c.p. crystal structure. The (1 1 1) and (2 0 0) diffraction peaks of the α phase in the bulk part of the specimen appeared at 2θ angles of 38.5° and 44.8° after the creep test at 150 °C, while the (1 0 $\bar{1}$ 0) and (0 0 0 2) diffraction peaks

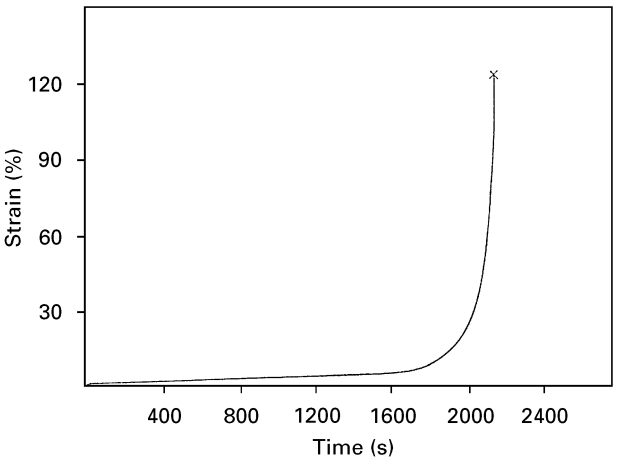

Figure 1 Creep curve of the furnace-cooled eutectoid Zn–Al alloy.

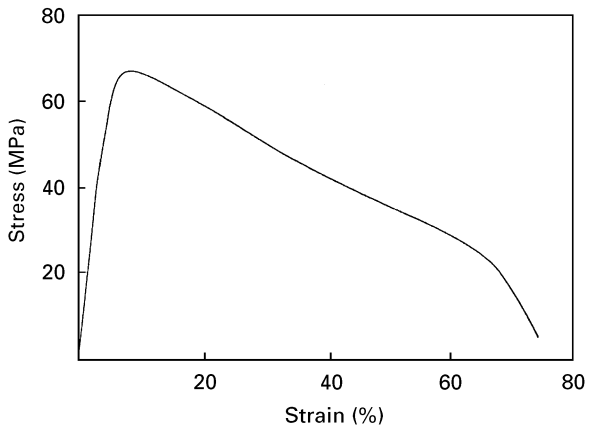

Figure 2 Stress–strain curve of the furnace-cooled eutectoid Zn–Al alloy.

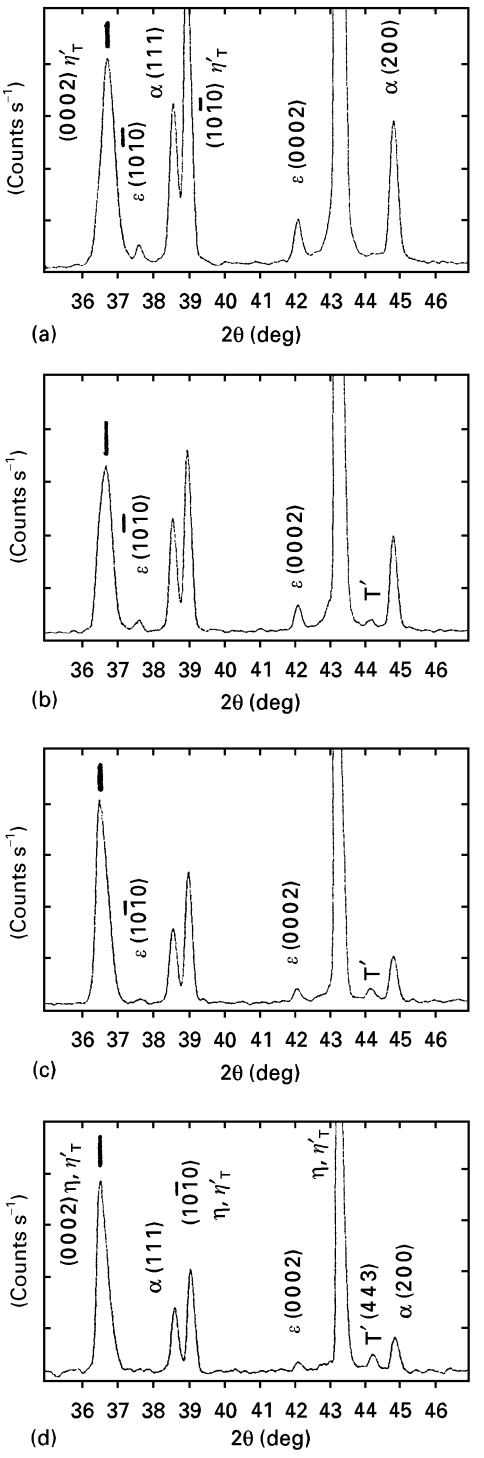

Figure 3 X-ray diffractograms of various parts of the furnace-cooled eutectoid Zn–Al alloy specimen after creep testing at 150 °C: (a) bulk part of the specimen; (b), (c) joint part of the specimen (neck zone + rupture part); (d) rupture part of the specimen

of the ε phase were at 2θ angles of 37.6° and 42.1°. The (0 0 0 2), (1 0 $\bar{1}$ 0) and (1 0 $\bar{1}$ 1) diffraction peaks of the η'_T phase in the bulk part of the tested specimen appeared at 36.7°, 39.0° and 43.3°, respectively. The (10$\bar{1}$1) diffraction peaks of the η'_T and ε phases overlapped at 43.3°. The X-ray diffractogram of the bulk part of the creep tested specimen is shown in Fig. 3a.

Shown in Figs 3b and c are the X-ray diffractograms of the joint parts of the neck zone and the rupture part of the creep-tested specimen. It was observed that, on approaching the rupture part of the specimen, the X-ray diffraction of the ε phase decreased gradually in intensity, while the characteristic X-ray diffraction of the T′ phase occurred and gradually increased in intensity at $2\theta = 44.3°$. The intensity of X-ray diffraction of the T′ phase increased to a maximum in the rupture part of the tested specimen, as shown in Figs 3c and d.

Also the shift of the (0 0 0 2) X-ray diffraction peak of the metastable phase η'_T was observed from a 2θ angle of 36.8° in the bulk part of the tested specimen to the smaller 2θ angle of 36.6° in the rupture part of the tested specimen; accordingly the *d* spacing of the (0 0 0 2) crystal plane increased from 0.2443 nm in the bulk part of the specimen to 0.244 nm and 0.2453 nm in the joint parts of the neck zone and rupture part and finally increased to 0.2456 nm in the rupture part of the specimen, as shown in Fig. 3

3.3. Scanning electron microscopy observation

The back-scattered scanning electron micrographs of both the bulk part and the rupture part of the specimen after creep testing at 150 °C are shown in Figs 4 and 5.

The bulk part of the specimen after creep testing consisted of a major coarsened lamellar structure (thickness of lamellae, about 0.4 μm), Zn-rich h.c.p. phase η'_T particles, diameter about 5 μm and a fine lamellar structure (thickness of lamellae, about 0.14 μm), where the light image was Zn-rich h.c.p. η'_T phase and the dark image was Al-rich f.c.c. α phase, as shown in Fig. 4.

In the rupture part of the specimen a spheroidized microstructure (diameter, about 0.6 μm) was observed in the original coarsened lamellar structure, except those aligned vertically to the tensile creep direction arrowed in Fig. 5, in addition to the fine lamellar structure. Shown in Fig. 5b is the microstructure very near the rupture tip zone, where most lamellar structures become parallel to the tensile creep direction under high extra strain.

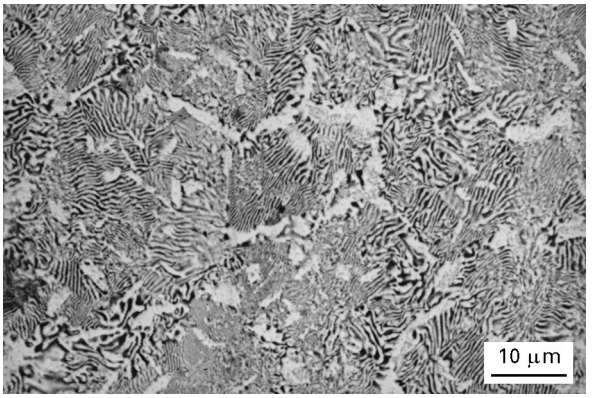

Figure 4 Scanning electron micrograph of the bulk part of the specimen after creep testing at 150 °C. (Magnification, 700×.)

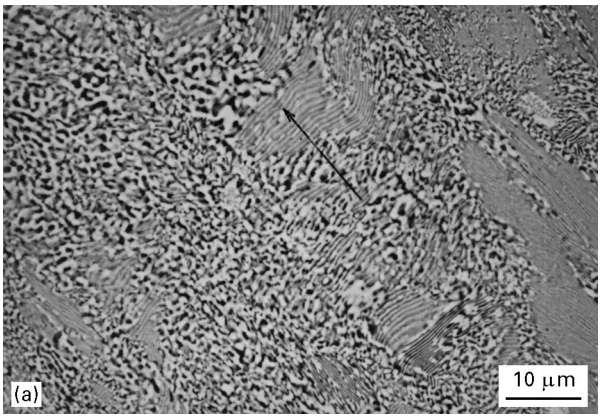

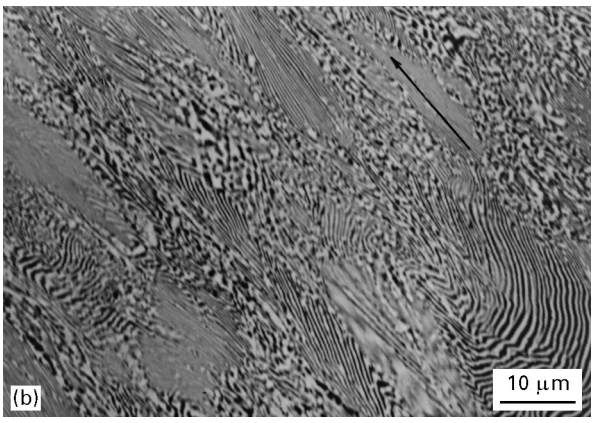

Figure 5 Scanning electron micrographs of the rupture part of the specimen after creep testing at 150 °C: (a) coarsened lamellar structure spheroidized except for those lamellae aligned vertically to the direction of creep; (b) very close to the rupture tip, showing all the lamellar structures approaching the direction of creep.

4. Discussion

4.1. Microstructure and phase relationships of the furnace-cooled alloy before creep testing

After solution treatment for 4 days at 350 °C, the eutectoid alloy consisted of two phases β and ε phases, as shown in the X-ray diffractogram of the solution treated and quenched specimen of the alloy, Fig. 6. The β phase was Zn-rich phase of fcc crystal structure, ε phase was h.c.p Zn_4Cu phase. Under equilibrium condition, below 276 °C β phase decomposed, and ε phase disappeared below 268 °C [4–6]. During furnace cooling, these three phases became metastable. The metastable phase β'_s decomposed via a cellular reaction and decomposed, $\beta'_s \rightarrow \alpha'_T + \varepsilon + \eta$, as a discontinuous precipitation at grain boundaries [6–8]. The metastable phase ε did not decompose and appeared as light contrast particles in the furnace

cooled alloy. During furnace cooling, the η phase became metastable phase η'_{FC}, with a characteristic (0 0 0 2) d-spacing of 0.2437 nm, less than that from the final stable state, 0.2457 nm. The X-ray diffraction results showed three phases α, ε and η'_{FC} co-existed in the alloy, as shown in Fig. 3.

4.2. Creep-induced microstructural change and phase transformations

During tensile creep testing at 150 °C, the bulk part of the specimen underwent a thermal treatment, i.e., ageing at 150 °C, while the rupture part and the neck zone of the specimen suffered a thermal–mechanical treatment, i.e., ageing at 150 °C + extra tension. As shown in Figs 4 and 5, the microstructural change and phase transformation were quite different. Both the decomposed α'_s phase and β'_s phase decomposed further to form a fine lamellar structure and a coarsened lamellar structure both derived in the bulk part of the specimen.

Under the concentrated high strain induced by tensile creep, the coarsened lamellar structure, except for the lamellae aligned vertically to the creep direction, spheroidized into fine particles of 0.5–0.8 μm diameter, and the fine lamellae kept the original structure after creep testing, shown in Fig. 5.

Accompanying the microstructural changes, two phase transformations occurred during creep testing. The metastable η'_T phase decomposed, with a characteristic shift of the (0 0 0 2) X-ray diffraction peak from 36.8° to the smaller 2θ angle of 36.6°; accordingly the *d* spacing of the (0 0 0 2) crystal plane increased from 0.2443 nm in the bulk part of the specimen to 0.2456 nm in the rupture part of the specimen, as shown in Fig. 3.

In the previous investigation on ageing characteristics of the solution-treatment-quenched, as-cast and extruded eutectoid Zn–Al-based alloy, it was determined that the metastable ε phase decomposed during prolonged ageing in the four-phase transformation, $\alpha_f + \varepsilon \rightarrow T' + \eta$ [7–18]. From the X-ray diffractograms of the bulk part, joint part (neck zone + rupture part) and rupture part of the specimen, shown in Fig. 3, it was detected that the X-ray diffraction peaks of the ε phase decreased in intensity from the bulk part of the rupture part of the specimen after creep testing; accordingly there was an accompanying increase in intensity of the X-ray diffraction of T′ phase. This implied that the ε phase decomposed during creep at 150 °C by the four-phase transformation, $\alpha_f + \varepsilon \rightarrow T' + \eta$, as observed in previous investigations [7–18]. It was obviously concluded that the four-phase transformation occurred in the furnace-cooled eutectoid Zn–Al alloy by further inducing extra tension during creep, i.e., the extra strain induced by creep could result in phase transformations which occur in a thermal treatment, i.e., ageing process.

The above-discussed microstructural change and phase transformation occurring in the furnace-cooled eutectoid Zn–Al alloy during tensile creep at 150 °C could be described schematically as follows:

furnance-cooled eutectoid Zn–Al alloy (consisting of three phases α, ε and η'_T)

(a) 150 °C ageing

→ decomposition of both α'_s and β'_s resulting in the formation of both fine and coarsened lamellar structures, and decomposition of η'_{Fc} (bulk part of the creep specimen)

(b) 150 °C ageing + tensile creep

→ partial spheroidization and decomposition of both η'_{Fc} and ε (rupture part of the creep specimen)

4.3. Microstructure dependence of creep behaviour

From the creep curve and the stress–strain curve of the furnace-cooled eutectoid alloy, shown in Figs 1 and 2, it was found that the furnace-cooled eutectoid Zn–Al alloy possessed fairly good tensile ductility and creep resistance.

It is recognized that better ductility of metals and alloys requires a fine stable grain size and adequate temperature. For the long-term tensile creep properties, it is necessary for the material to possess some stable microstructure which would withstand well the extra stress in combination with good ductility.

It was found that the furnace-cooled eutectoid Zn–Al alloy consisted mainly of the coarsened lamellar structure derived from the decomposed β'_s phase. During tensile creep, the coarsened lamellae of 0.4 μm thickness, except for those aligned vertically to the direction of the creep direction, spheroidized gradually with increasing extra strain into fine particles of about 0.5–0.8 μm diameter, providing a major spheroidized structure which plays an important part in the better ductility of the alloy by easy displacement of individual grains through the process of grain-boundary sliding.

It was concluded that there were several transitional phases, such as α''_m and α'_m phases, which existed during the ageing of Zn–Al-based alloys (of monotectoid and eutectoid compositions) [8, 11, 19]. It was also reported that the decomposition of the Zn-rich supersaturated β'_s phase was more rapid than that of Al-rich α'_s phase because Al has a much lower diffusion coefficient than Zn does [8, 11, 19]. While the β'_s phase decomposed almost completely and became the coarsened lamellar structure during creep testing at 150 °C, the α'_s phase had not yet totally decomposed and appeared as a fine lamellar structure. The transitional phases α''_m and α'_m in the decomposed α'_s phase played an important part in strengthening the material [8, 11, 19].

The strengthened fine lamellar structure derived from the α phase in the furnace-cooled eutectoid Zn–Al alloy, containing the transitional phases α''_m and α'_m, withstood the creep-induced extra stress. An adequate balance must be maintained between strength and ductility, i.e., between the major spheroidized structure and the strengthened fine lamellar structure, with an enhanced creep resistance and also creep

rupture strength of the furnace-cooled eutectod Zn–Al alloy.

5. Conclusions

The conclusions are as follows.

1. When the furnace-cooled eutectoid Zn–Al alloy 76 wt% Zn–22 wt% Al–2 wt% Cu deformed at a minimum creep rate of $7.2 \times 10^{-3}\ s^{-1}$ under 30 MPa stress at 150 °C, the creep specimen ruptured after the strain reached 135.0% and the time to rupture was 2177 s.
2. Decomposition of the metastable phase η'_T and the four-phase transformation, $\alpha_f + \varepsilon \rightarrow T' + \eta$, occurred in the furnace-cooled eutectoid alloy during creep at 150 °C.
3. The coarsened lamellar structure derived from the decomposed β'_s phase except for those lamellae aligned vertically to the creep direction, changed into a spheroidized structure during creep at 150 °C.
4. The furnace-cooled eutectoid Zn–Al alloy consisted mainly of decomposed β'_s phase, which provided a major spheroidized structure and much enhanced the tensile ductility of the alloy during tensile creep at 150 °C. In combination with the spheroidized structure, the strengthened fine lamellar structure withstood the creep-induced extra stress and improved the creep resistance and creep rupture strength of the furnace-cooled eutectoid Zn–Al alloy.

Acknowledgements

The authors are grateful to Lettuce Baños, Antonio Caballero, L. Bucio, A. Arizmendi, Jose Guzman and Afredo Maciel Cerda for their help in the experimental work.

Referenes

1. C. A. LOONG, in "Proceedings of the 25th Canadian Institute of Mine and Metallurgy (CIM) Conference", Toronto, 1986 (1986) p. 157.
2. M. DUTMAN and S. MURPHY, *Z. Metalkde* **82** (1991) 129.
3. *Idem*., in " Proceedings of the Third International Conference on Zn–Al alloys", Mexico City, 1994, edited by G. Torres-Villaseñor, Y. H. Zhu and C. Piña (1994) p. 59.
4. S. MURPHY, J. Metal Sci. **9** (1975) 163.
5. Y. H. ZHU, *Chin. J. Met. Sci. Technol.* **5** (1989) 113.
6. *Idem*., *ibid.* **2** (1986) 105.
7. *Idem*., in "Proceedings of the Third International Conference on Zn–Al alloys", Mexico City, 1994 edited by G. Torres-Villaseñor, Y. H. Zhu and C. Piña (1994) p. 77.
8. *Idem*., *Chin. J. Met. Sci. Technol.* **6** (1990) 125.
9. Y. H. ZHU and E. OROZCO, *Metall. Mater. Trans. A*, **26** (1995) 2611.
10. Y. H. ZHU and S. MURPHY, *Chin. J. Met. Sci. Technol.* **3** (1987) 261.
11. Y. H. ZHU, G. TORRES-VILLASEÑOR and C. PIÑA, J. Mater. Sci. **29** (1994) 1549.
12. Y. H. ZHU and F. E. GOODWIN, *Mater. Sci. Technol.* **10** (1994) 121.
13. *Idem*., *J. Mater. Res.* **10** (1995) 1927.
14. Y. H. ZHU, B. YAN and W. HUANG, in "Proceedings of the International Symposium on Zn–Al Cast Alloys", Toronto, 1986, edited by G. P. Lewis, R. J. Barnhurst and C. A. Loong (1986) p. 23.
15. Y. H. ZHU, *Shanghai Metals* (*Nonferrous Fascicule*) **11** (1990) 1.
16. Y. H. ZHU, W. HUANG and B. YAN, *ibid.* **9** (1988) 1.
17. N. MYKURA, S. MURPHY and Y. H. ZHU, in "Proceedings of the Materials Research Society Annual Conference", Vol. 21, (Elsevier, Amsterdam, 1984) p. 841.
18. Y. H. ZHU, T. SAVANSKAN and S. MURPHY, in "Proceedings of the Materials Research Society Annual Conference", Vol. 21 (Elsevier, Amsterdam, 1984) p. 835.
19. Y. H. ZHU, Journal Materials Research Vol. 11, 1996, 3, 593.

Received 8 December 1995
and accepted 10 March 1997